Supplementary Material

Phosphorescent chemosensor for Hg^{2+} based on iridium(III) complex coordinated with 4-phenylquinazoline and sodium carbazole dithiocarbamate

Qunbo Mei, [a]* Yujie Shi, [a] Qingfang Hua, [a] Bihai Tong[b]*

[a] *Key Laboratory for Organic Electronics and Information Displays & Institute of Advanced Materials(IAM), Jiangsu National Synergetic Innovation Center for Advanced Materials (SICAM), Nanjing University of Posts & Telecommunications, 9 Wenyuan Road, Nanjing 210023, China.*
[b] *College of Metallurgy and Resources, Anhui University of Technology, Ma'anshan, Anhui 243002, P. R. China*
∗ *Corresponding author. e-mail: iamqbmei@njupt.edu.cn; tongbihai@ahut.edu.cn*

Contents:

Detection limit:

The detection limit was determined from the fluorescence titration data based on a reported method.[1] The fluorescence spectrum of probe **Ir(pqz)$_2$(cdc)** was measured by six times and the standard deviation of blank measurement was achieved. To gain the slop, the fluorescent intensity data at 562 nm was plotted as a concentration of Hg^{2+}. So the detection limit was calculated with the following equation:

$$\text{Detection limit}=3\sigma/K$$

Where σ is the standard deviation of blank measurement, and K is the slop between the fluorescence versus Hg^{2+} concentration.

There was a good linearity at micro molar concentration levels between fluorescent intensity data at 562 nm and concentrations of Hg^{2+} in the range from 6×10^{-6} M to 24×10^{-6} M, indicating the probe **Ir(pqz)$_2$(cdc)** can detect quantitatively relevant concentrations of Hg^{2+}. The linear equation was found to be y=31.438x-106.557(R=0.998), where y is the fluorescent intensity data at 562 nm measured at a given Hg^{2+} concentration and x represents the concentration of Hg^{2+} added. So the detection limit for Hg^{2+} was calculated to be 25nM(Detection limit=3σ/K=0.801/31.438$\times10^{-6}$ M ≈ 25nM).

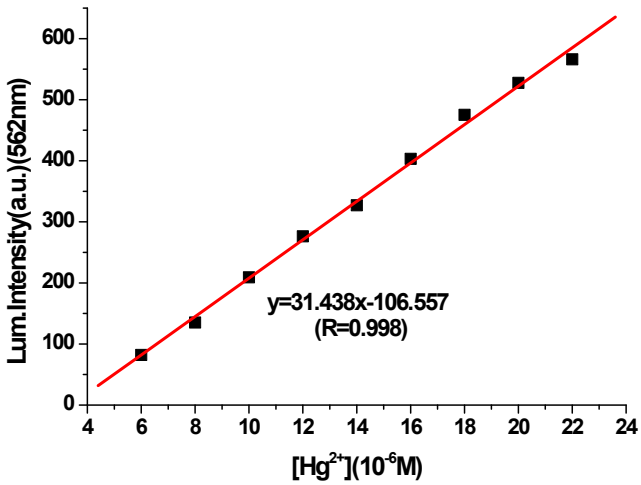

Figure S1. Normalized response of fluorescence signal of **Ir(pqz)$_2$(cdc)** in DCM+ MeCN (V_{DCM}:V_{MeCN}=10:1, 2.0×10^{-5} M) in the presence of increasing amount of Hg^{2+} (6×10^{-6} M to 24×10^{-6} M) predissolved in acetonitrile. (λ_{ex}=360nm; λ_{em}=562nm).

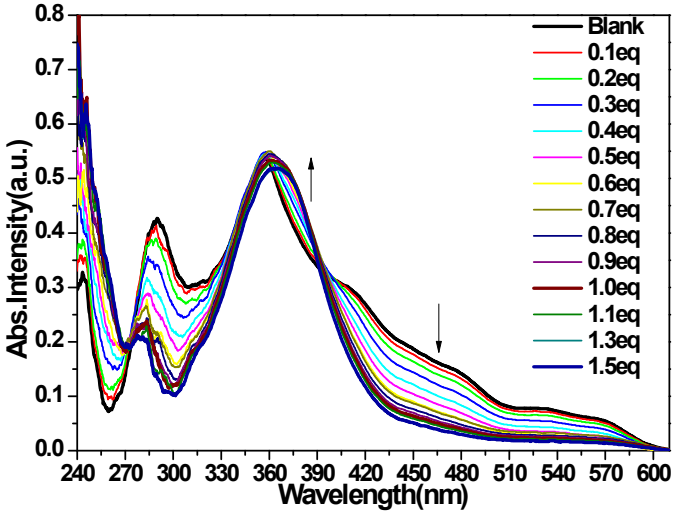

Figure S2. UV-vis spectra of **Ir(pqz)$_2$(cdc)** in DCM+ THF (V_{DCM}:V_{THF}=10:1, c = 2.0×10^{-5} M) in the presence of increasing amount of $Hg(ClO_4)_2$ (0-1.5 equiv) predissolved in THF. Arrows indicate the absorptions that increase (up) and decrease (down) during the titration experiments.

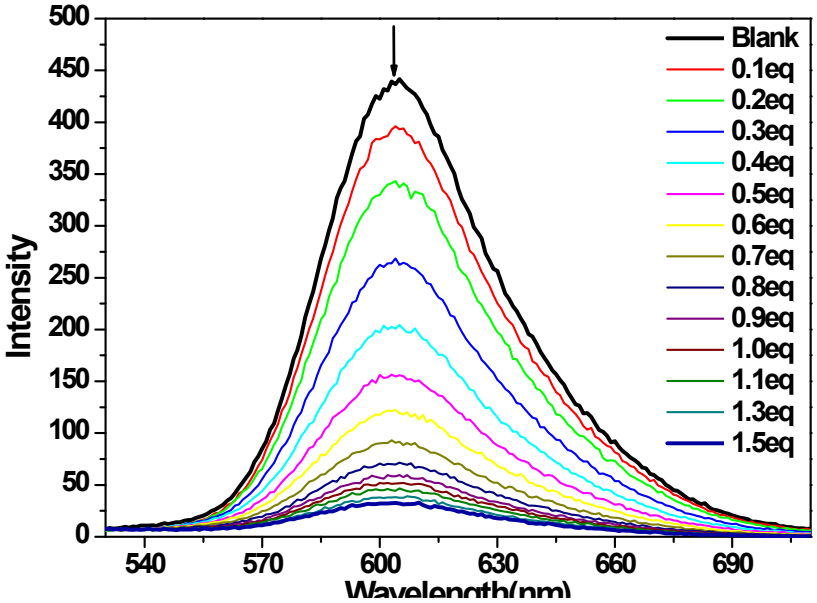

Figure S3. Fluorescence emission spectra of **Ir(pqz)$_2$(cdc)** in DCM+ THF (V_{DCM}:V_{THF}=10:1, 2.0×10^{-5} M, λ_{ex}=360nm) in the presence of increasing amount of Hg^{2+} (0-1.5 equiv) predissolved in THF.

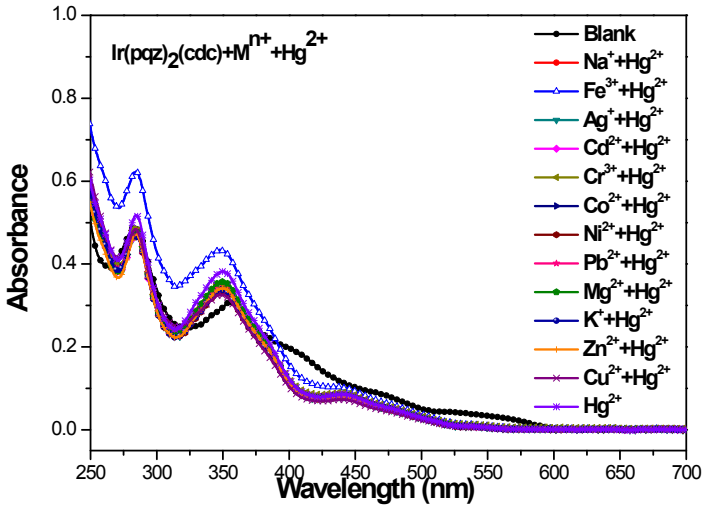

Figure S4. UV-vis spectra of **Ir(pqz)$_2$(cdc)** (c = 2.0×10^{-5}) in the presence of 2 equiv of Hg^{2+} and 2 equiv of other metal ions at the same time in DCM+ MeCN(V_{DCM}:V_{MeCN}=10:1). Na^+, Fe^{3+}, Ag^+, Cd^{2+}, Cr^{3+}, Co^{2+}, Ni^{2+}, Pb^{2+}, Mg^{2+}, K^+, Zn^{2+} and Cu^{2+} were added, respectively.

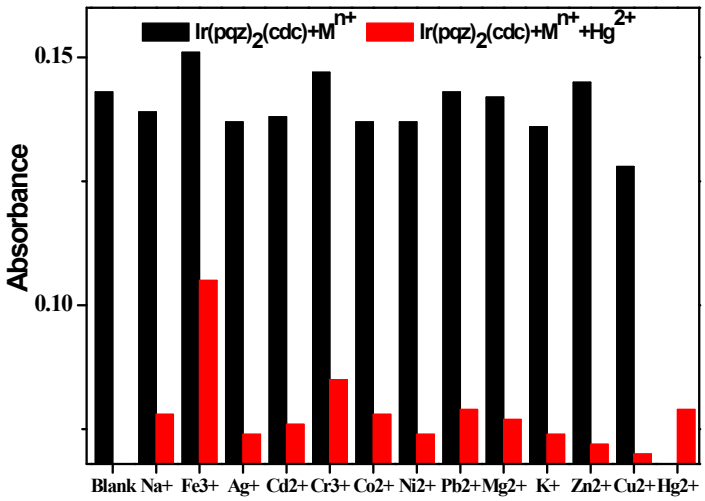

Figure S5. UV-vis absorption responses of **Ir(pqz)$_2$(cdc)** in DCM+ MeCN (V_{DCM}:V_{MeCN}=10:1, 2.0×10^{-5} M) to various 2 equiv of metal ions. Bars represent the final ($A_{(425nm)}$) absorption intensity. The black bars represent the free **Ir(pqz)$_2$(cdc)** solution and the addition of various metal ions (2 equiv) to a solution of **Ir(pqz)$_2$(cdc)**. The red bars represent the change of the absorption intensity that occurs upon the subsequent addition of 2 equiv of Hg^{2+} to the above solution.

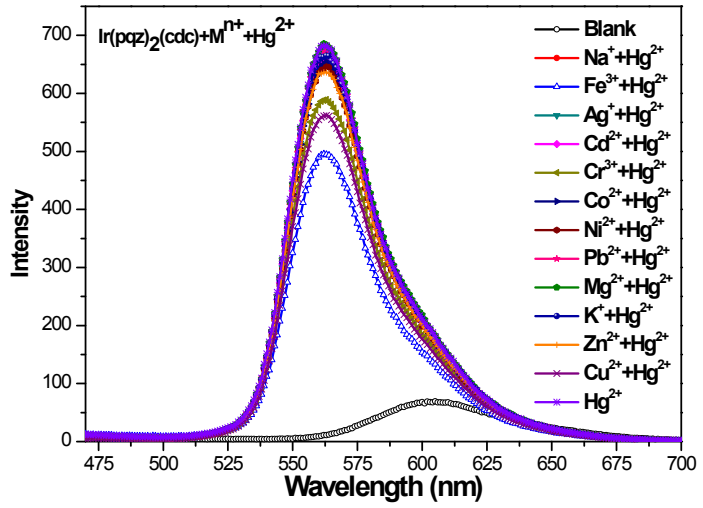

Figure S6. Emission spectra of **Ir(pqz)$_2$(cdc)** (c = 2.0×10^{-5} M) in the presence of 2 equiv of Hg^{2+} and 2 equiv of other metal ions at the same time in DCM+ MeCN(V_{DCM}:V_{MeCN}=10:1). Na^+, Fe^{3+}, Ag^+, Cd^{2+}, Cr^{3+}, Co^{2+}, Ni^{2+}, Pb^{2+}, Mg^{2+}, K^+, Zn^{2+} and Cu^{2+} were added, respectively.

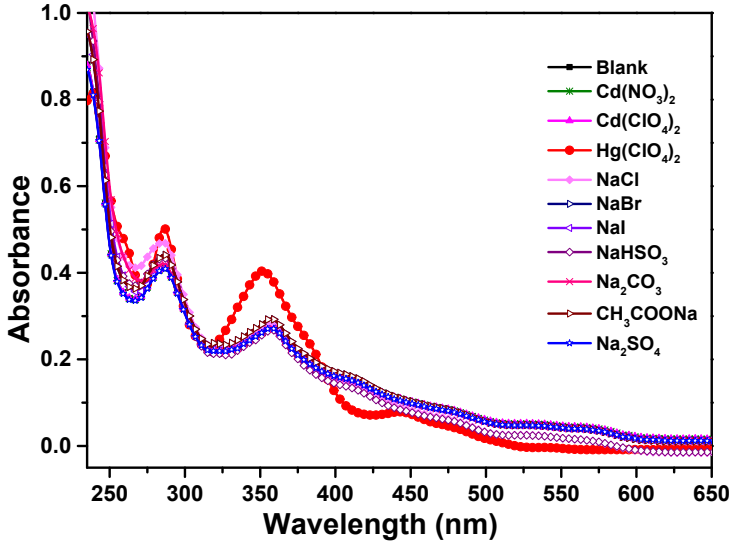

(a)

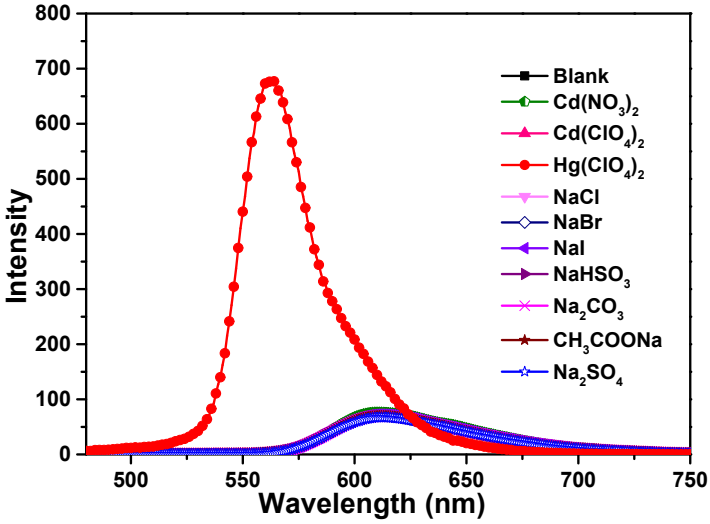

(b)

Figure S7. (a) UV-vis spectra of **Ir(pqz)$_2$(cdc)** (c = 2.0×10^{-5} M) in the presence of main group metal salt and transition metal salt with different anions (2.0 equiv) in DCM+ MeCN(V_{DCM}:V_{MeCN}=10:1). (b) Emission spectra of **Ir(pqz)$_2$(cdc)** (c = 2.0×10^{-5} M) in the presence of main group metal salt and transition metal salt with different anions (2.0 equiv) in DCM+ MeCN(V_{DCM}:V_{MeCN}=10:1).

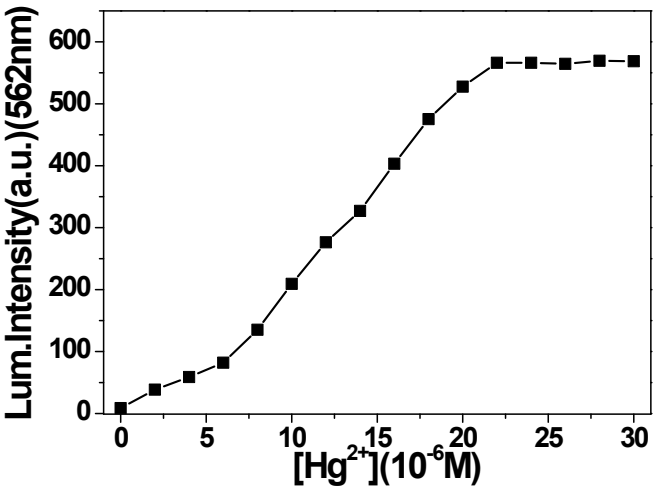

Figure S8. Fluorescence intensity of **Ir(pqz)$_2$(cdc)** in DCM + MeCN (V_{DCM}:V_{MeCN}=10:1, 2.0×10^{-5} M) contained different concentrations of Hg^{2+} (0-1.5 equiv) at λ_{em} = 562 nm.

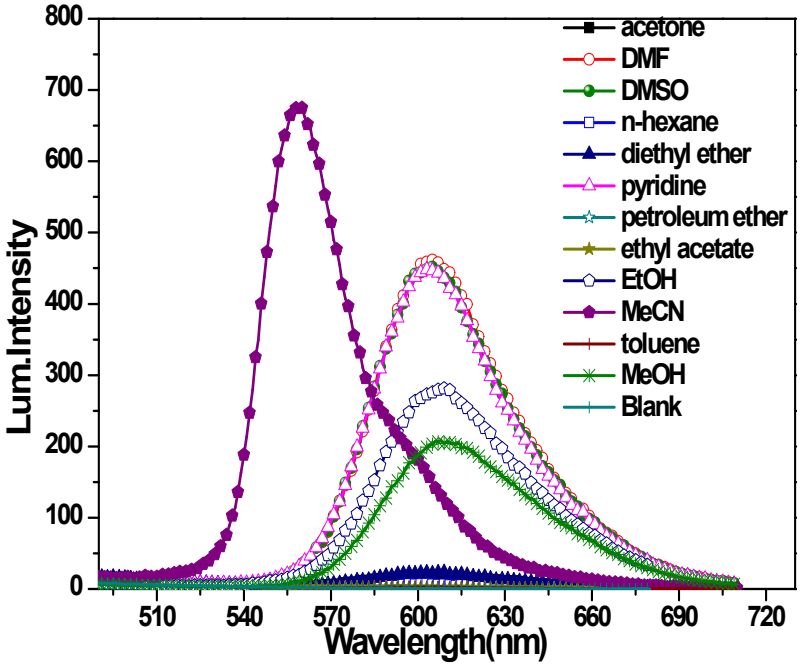

Figure S9. Emission spectra of **Ir(pqz)$_2$(cdc)** (c = 2.0×10^{-5} M) in the presence of 2 equiv of Hg^{2+} in 2 mL DCM and the addition of various solvents(10μL). acetone, DMF, DMSO, n-hexane, diethyl ether, pyridine, petroleum ether, ethyl acetate, EtOH, acetonitrile, toluene, MeOH and Blank were added, respectively.

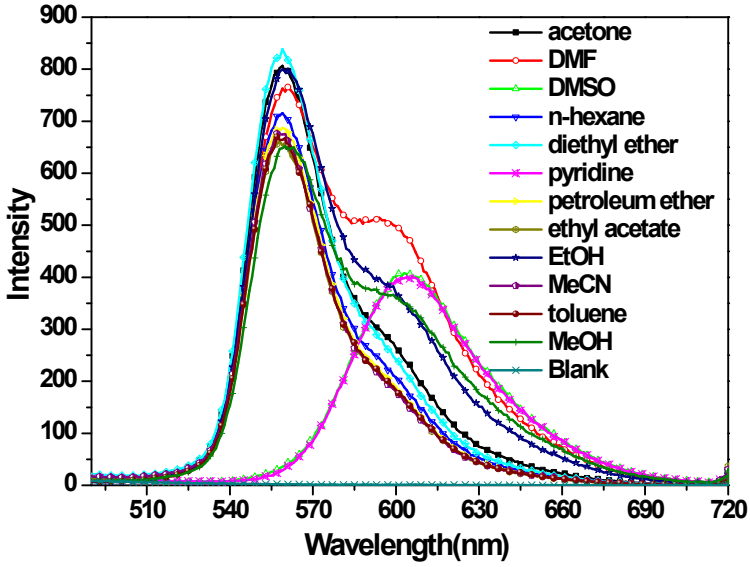

Figure S10. Emission spectra of **Ir(pqz)$_2$(cdc)** (c = 2.0×10^{-5} M) with 2 equiv of Hg^{2+} in the presence of MeCN(10μL) and other various solvents(10μL) at the same time in 2 mL DCM solution.

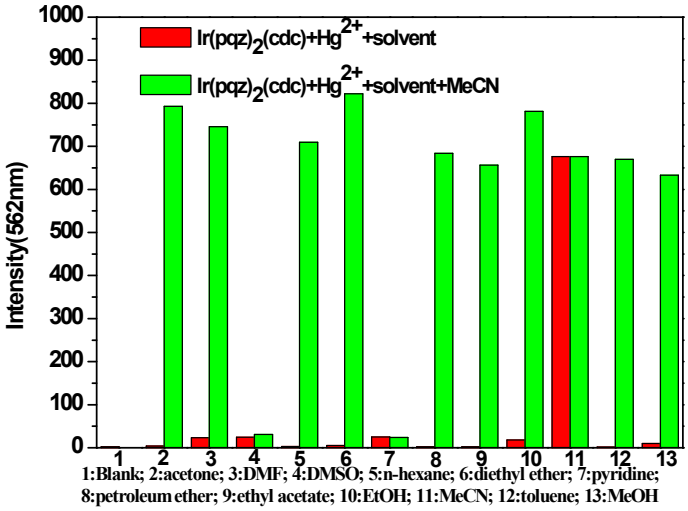

Figure S11. Fluorescence responses of **Ir(pqz)$_2$(cdc)** (c = 2.0×10^{-5} M) with 2 equiv of Hg^{2+} in the presence of 10μL various solvents in 2 mL DCM solution. Bars represent the final ($I_{(562nm)}$) emission intensity. The red bars represent the addition of various solvents (10μL) to a solution of **Ir(pqz)$_2$(cdc)** with 2 equiv of Hg^{2+}. The green bars represent the change of the emission intensity that occurs upon the subsequent addition of 10μL MeCN to the above solution.

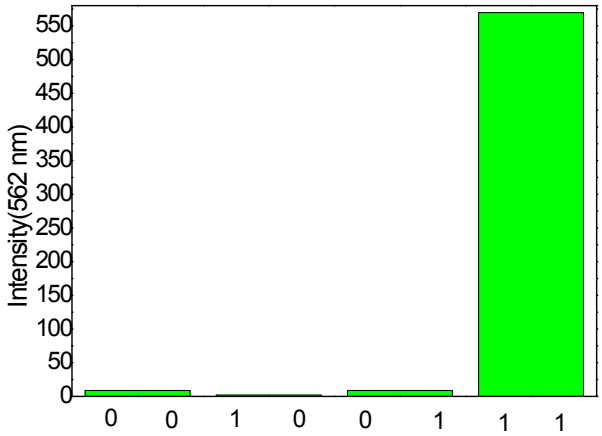

Figure S12. Fluorescence output of Ir(pqz)$_2$(cdc) (2.0×10^{-5} M) in the presence of chemical inputs (Hg^{2+} (1.5 equiv) and MeCN (1 μL) (When the fluorescence intensity at 562 nm was less than 10 marked 0, on the contrary, marked 1)

Table S1. Crystal data and structure refinement for **Ir(pqz)$_2$(cdc)**.

Identification code	**Ir(pqz)$_2$(cdc)**
Empirical formula	C_{41} H_{26} Ir N_5 S_2
Formula weight	844.99
Temperature	293(2) K
Wavelength	0.71073 Å
Crystal system, space group	Triclinic, P-1

Unit cell dimensions	a = 11.4807(13) Å alpha = 64.3290(10) deg. b = 12.9220(14) Å beta = 75.1090(10) deg. c = 13.0863(15) Å gamma = 74.1730(10) deg.
Volume	1661.7(3) $Å^3$
Z, Calculated density	2, 1.689 Mg/m^3
Absorption coefficient	4.182 mm^{-1}
F(000)	832
Crystal size	0.65 x 0.57 x 0.13 mm
Theta range for data collection	2.35 to 27.45 deg.
Limiting indices	-14<=h<=13, -16<=k<=15, -15<=l<=16
Reflections collected / unique	10302 / 7278 [R(int) = 0.0183]
Completeness to theta = 27.45	96.0 %
Absorption correction	Semi-empirical from equivalents
Max. and min. transmission	0.6124 and 0.1719
Refinement method	Full-matrix least-squares on F^2
Data / restraints / parameters	7278 / 0 / 442
Goodness-of-fit on F^2	1.062
Final R indices [I>2sigma(I)]	R1 = 0.0265, wR2 = 0.0672
R indices (all data)	R1 = 0.0292, wR2 = 0.0687
Largest diff. peak and hole	2.211 and -0.989 e. $Å^{-3}$

Table S2. Bond lengths [Å] and angles [deg] for **Ir(pqz)$_2$(cdc)**.

Ir(1)-C(21)	1.994(3)
Ir(1)-C(16)	2.010(3)
Ir(1)-N(4)	2.041(3)
Ir(1)-N(2)	2.049(3)
Ir(1)-S(2)	2.4474(8)
Ir(1)-S(1)	2.4823(8)
C(21)-Ir(1)-C(16)	86.78(12)
C(21)-Ir(1)-N(4)	78.77(11)
C(16)-Ir(1)-N(4)	93.68(11)
C(21)-Ir(1)-N(2)	94.64(11)
C(16)-Ir(1)-N(2)	78.93(11)
N(4)-Ir(1)-N(2)	170.45(9)
C(21)-Ir(1)-S(2)	98.59(8)
C(16)-Ir(1)-S(2)	174.42(8)
N(4)-Ir(1)-S(2)	88.86(8)
N(2)-Ir(1)-S(2)	99.03(7)
C(21)-Ir(1)-S(1)	169.21(8)
C(16)-Ir(1)-S(1)	103.97(9)
N(4)-Ir(1)-S(1)	99.33(8)
N(2)-Ir(1)-S(1)	88.41(8)
S(2)-Ir(1)-S(1)	70.68(3)

Table S3 The emission intensity ($I_{562\ nm}$) in the presence of various solvents(10 μL).

Number	Solvent	Emission intensity($I_{562\ nm}$)[a]
1	Blank	2.365
2	acetone	3.809
3	DMF	23.302
4	DMSO	24.72
5	n-hexane	2.631
6	diethyl ether	5.441
7	pyridine	25.239
8	petroleum ether	2.284
9	ethyl acetate	2.141
10	EtOH	18.291
11	MeCN	676.395
12	toluene	1.764
13	MeOH	9.824

[a] Fluorescence responses of **Ir(pqz)$_2$(cdc)** (2.0×10^{-5} M) in the presence of 2 equiv of Hg^{2+} in 2 mL DCM in the presence of various solvents(10 μL).

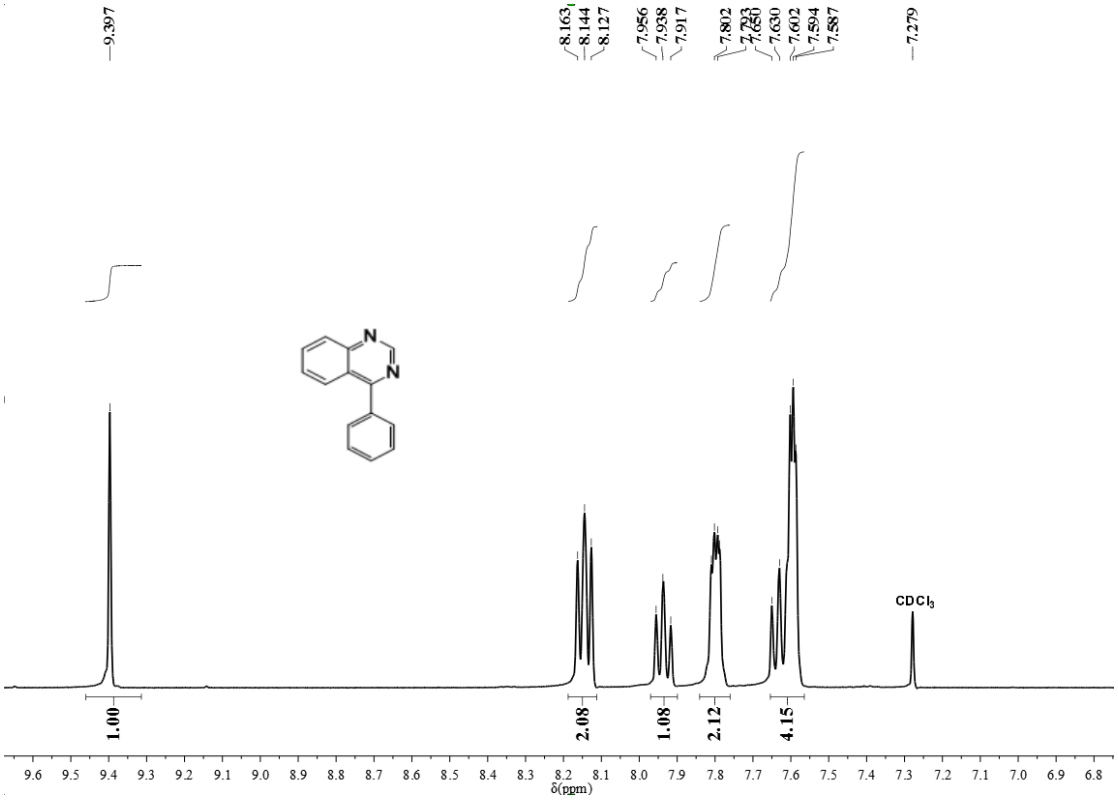

Figure S13. ^{1}H NMR of **pqzH** in $CDCl_3$

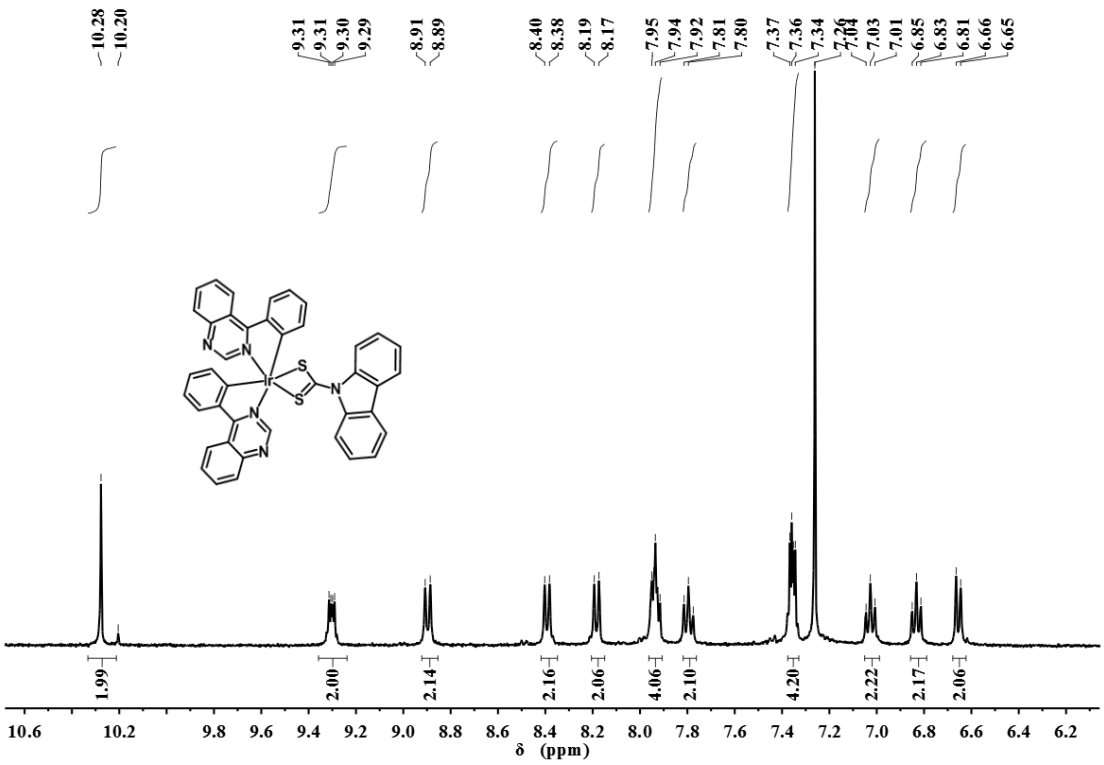

Figure S14. ^{1}H NMR of **Ir(pqz)$_2$(cdc)** in $CDCl_3$

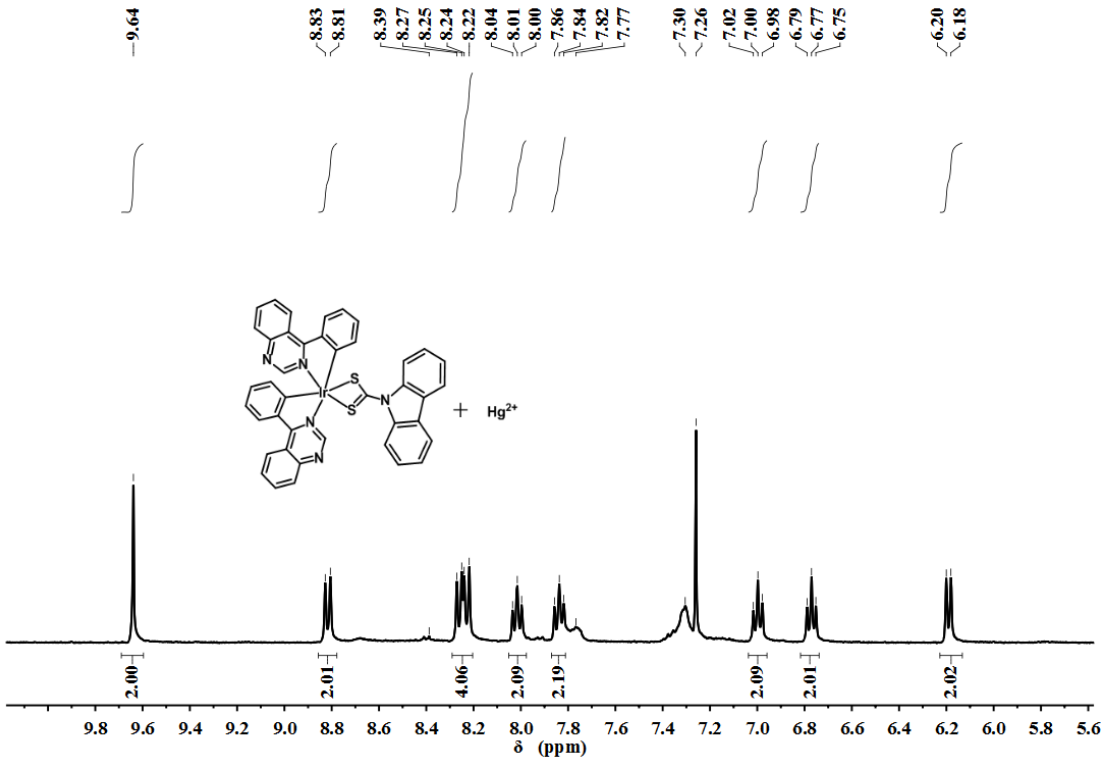

Figure S15. ^{1}H NMR of **Ir(pqz)$_2$(cdc)** with excessive of **Hg^{2+}** in $CDCl_3$

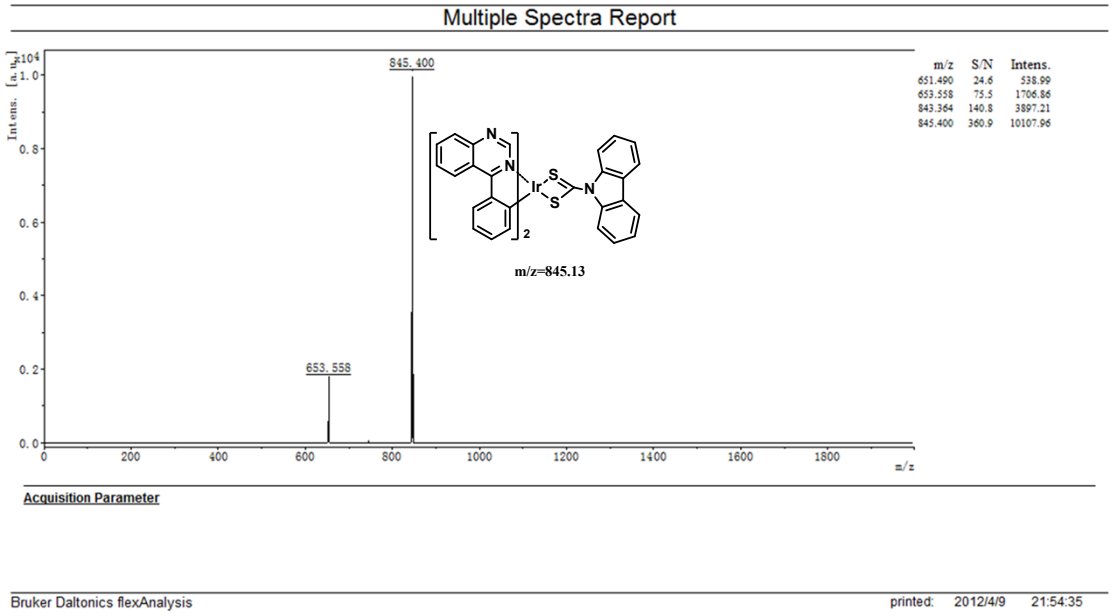

Figure S16. MADIL-TOF mass spectrum of **Ir(pqz)$_2$(cdc)**

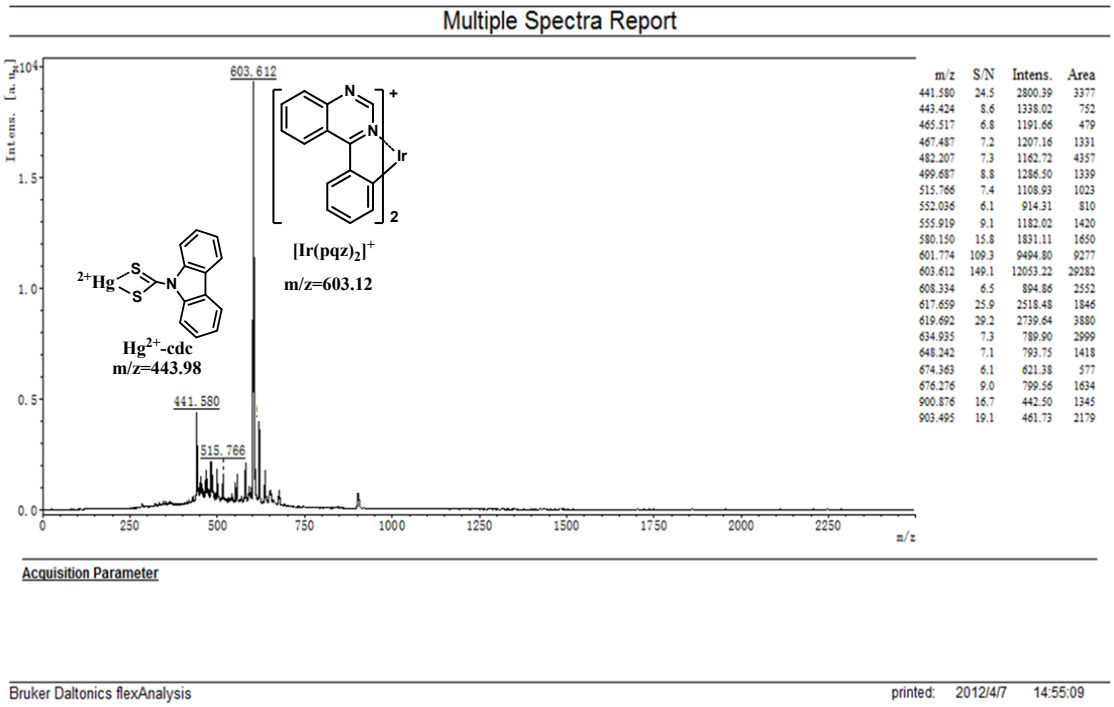

Figure S17. MADIL-TOF mass spectrum of **Ir(pqz)$_2$(cdc)** with excessive of Hg^{2+}

References:

1. (a) Yamin Li, Y.M.; Zhang, X.L.; Zhu, B.C.; Yan, J.L.; Xu, W.P. Analytical Sciences **2010**, 26, 1077; (b) Yang, X.F.; Wang, L.P.; Xu, H.M.; Zhao, M.L. Analytica Chimica Acta **2009**, 631, 91; (c) Yang, Y.; Jiang, J.H.; Shen, G.L.; Yu, R.Q. Analytica Chimica Acta **2009**, 636, 83; (d) Ma, Q.J.; Zhang, X.B.; Zhao, X.H.; Jin, Z.; Mao, G.J.; Shen, G.L.; Yu, R.Q. Analytica Chimica Acta **2010**, 663, 85.
2. (a) Kubo, Y.; Kato, M.; Misawa, Y.; Tokita, S. Tetrahedron Lett. **2004**, 45, 3769; (b) Yang, M.H.; Thirupathi, P.; Lee, K.H. Org. Lett. **2011**, 13, 5028.